

Fragility Functions for a Pervasive Unique Form of Construction in a Region with Very High Potential for Social Losses

B.D. Carey & R.P. Clarke

The University of the West Indies, St. Augustine, Trinidad and Tobago



15 WCEE
LISBOA 2012

Summary:

The twin-island republic of Trinidad and Tobago is fortunate to have an abundance of natural resources resulting in its being a major source of economic support for the English-speaking Caribbean. The economic stability of the Caribbean is threatened, via a domino effect, by the current prevalent form of residential structures in Trinidad and Tobago because of a lack of conformity with proper seismic design in an earthquake prone region (S_S of 0.9-1.3g). Fragility functions for typical two-storey residential structures were derived using Incremental Dynamic Analysis considering both aleatory and epistemic uncertainties. The selected ground motion records are compatible with spectra derived for the Caribbean region. Fragility functions for the structures are with respect to limit states of slight, moderate, extensive, and complete damage as well as out-of-plane dynamic instability. These fragility functions can be used for regional risk assessment hence the derivation of disaster mitigation and management plans thereby avoiding a major crisis in the Caribbean.

Keywords: Extended Incremental Dynamic Analysis, Epistemic Uncertainty, Unreinforced Masonry

1. INTRODUCTION

The Caribbean region is comprised of many territories. Thirteen of these are independent English-speaking states in an alliance called CARICOM (Caribbean Community). To enable greater economic integration, the CSME (CARICOM Single Market and Economy) is a collection of policies of relaxed restrictions to stimulate activity via free movement of entrepreneurs within CARICOM states. In CARICOM and the CSME Trinidad and Tobago is effectively the financial center being uniquely fortunate as the only state with oil and natural gas among its natural resources. The national income from oil and gas has been and continues to be invested in industrial and infrastructural development thereby supporting businesses that export goods to the other CARICOM states at very competitive rates. In many instances most of the goods in these states originate from businesses in Trinidad and Tobago making Trinidad and Tobago important to the quality of life in these territories. Trinidad and Tobago has targeted 2020 as the year it intends to achieve “developed country” status. However, its decision-makers and the population in general reside in homes that are inappropriate for an earthquake prone region and if the “design earthquake” were to occur, the Caribbean will suffer extensive losses not significantly different than the infamous Haiti earthquake of 2010.

At least eighty percent of the existing building stock in Trinidad and Tobago comprises of residential structures of four types as follows:

1. Single-storey unreinforced masonry (URM) residential structures where the type of URM is of 100mm thick clay tile, and the roof load is 0.3 to 0.5 kN/m². This represents about sixty percent of the total building stock.

2. Two-storey structures with the upper storey exactly the same as *Type 1*, but the lower storey of reinforced concrete (RC) frames supporting a cast in-situ reinforced concrete floor. The RC frame elements are not seismically detailed. For this type of structure the lower storey is not used, though there is generally an intention to enclose the area in future. Therefore the house can be visually described as a “house of stilts”.
3. The same as *Type 2* except that the lower storey is enclosed by infilling the spaces between the frames with the same URM tiles used for the upper storey.
4. The same as the “house on stilts” of *Type 2*, but the stilts are on the sloping surface of a hillside.

For each of these four structural types, a professional engineer is not involved in the construction phase in the vast majority of instances, and the design is based on “deemed-to-satisfy” provisions. Fragility curves for the *Type 1* structure were developed in a previous study (Clarke, 2010) and are excluded from this study. Figures 1 to 3 depict the structural models of house *Types 2 to 4*, respectively.

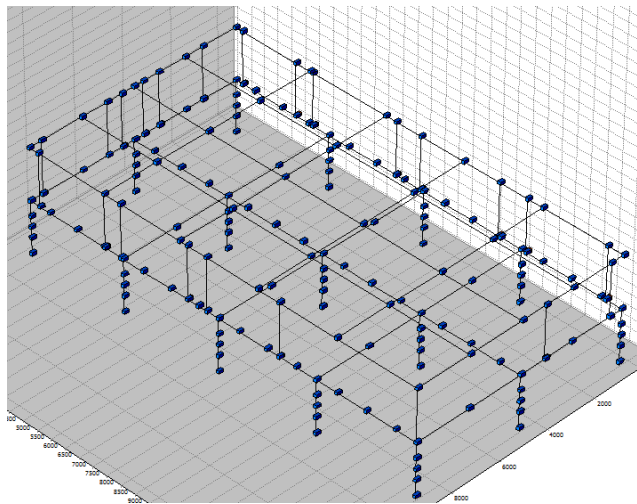


Figure 1. Mathematical Model for House *Type 2*

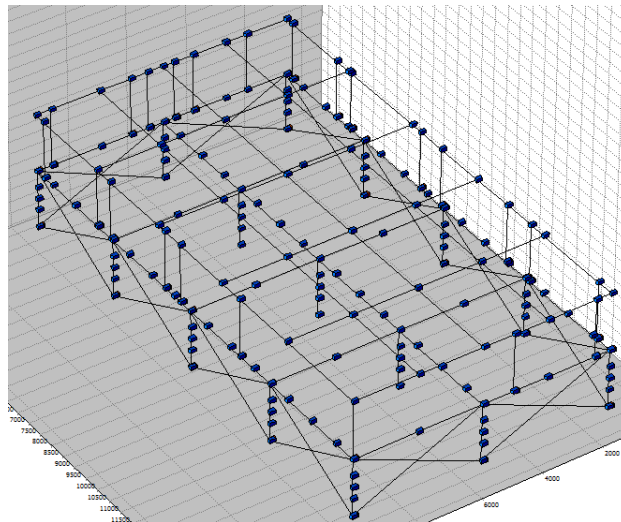


Figure 2. Mathematical Model for House *Type 3*

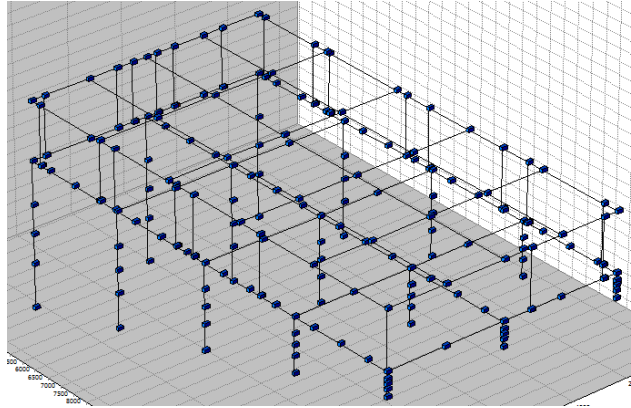


Figure 3. Mathematical Model for House *Type 4*

Given these types of buildings this situation is one of significant risk to the future development of Trinidad and Tobago and the English-speaking Caribbean. As a mitigation effort, a rehabilitation design for the *Type 1* structure was completed in 1998 based on the use of overlays. However, recent technological developments, largely due to the performance-based design paradigm, enable probabilistic assessment of the structure before and after rehabilitation, or loss estimates of entire towns given certain scenarios, and hence can enhance the decision-making process of the various stakeholders in ways previously unavailable. Probabilistic assessment and loss estimation methodologies have been developing rapidly in earthquake structural engineering over the past two decades and popular methods such as the PEER framework typically require the fragility curves for the structure (ATC, 2007). The Incremental Dynamic Analysis (IDA) method by Vamvatsikos and Cornell (2002) is associated with the PEER framework and can be used to determine the fragility curves. However, in many instances practical use of IDA has not included the epistemic uncertainty and judgment is frequently relied on to specify a value. A methodology for including the epistemic uncertainty was recently developed by Dolsek (2009) for use with IDA and is called Extended Incremental Dynamic Analysis (EIDA)

This paper presents the results of fragility analyses of the aforesaid house *Types 2,3, and 4* and the resulting fragility functions. Central to the fragility analysis is the use of the EIDA method based on nonlinear dynamic analysis of the structure.

2. STRUCTURAL MODELS

The typical form of residential construction has walls comprised of clay tile masonry units for both the load-bearing and the internal partition walls. These units are manufactured in accordance with ASTM C34 and are used with cells in the horizontal orientation. The clay tile unit is of dimensions 200 mm high by 300 mm long by 100 mm thick, with web and shell thicknesses of approximately 8 mm. The unit weighs 5.5 kg, and has a compressive strength (average of 5 units), of approximately 3.5 MPa.

Figures 1-3 show the layout of the typical two-storey residential structures in Trinidad and Tobago. Residential homes are commonly of rectangular plan, 9.0 m wide by 11.0 m long, and the storey height is 2.4 m. The lower storey is often comprised of a RC frame with members approximately 300mm by 300mm, and this frame supports a 100mm RC slab. The roof is of gable shape (though sometimes hipped) of slope 22 to 30 degrees from the horizontal. It is comprised of galvanized steel corrugated sheeting supported by 50 mm by 100 mm timber secondary beams, or 100 mm cold-steel Z-purlins. Further description of the typical construction techniques can be found Clarke (2010).

The lateral load resisting structural system of the upper storey as described above can therefore be classified as a box system of unreinforced masonry (URM) shear walls. URM shear wall structures are acknowledged to have four fundamental possible modes of response in the in-plane direction– flexural leading to toe compression failure, shear leading to diagonal tension failure, rocking, and sliding. The actual response is frequently a combination of these modes and the level of bearing stress on the wall is a very significant factor determining which mode will dominate the response. In the out-of-plane direction, after formation of a horizontal through-wall crack at the base, depending on the level of bearing stress, a stable rocking response is possible. However, there is a level of lateral displacement beyond which failure by dynamic instability will likely occur. Given the description of the structure, and considering test data on the in-plane response of a prototype of the wall (Clarke, 1998), the following presumptions regarding its behavior hence structural modeling are made:

1. Under significant lateral load the “toothed” connection of the internal to external walls will cause a vertical line of weakness in the external walls and separate them into a set of vertical elements, from ground level to the top of the wall, interconnected at the top by the ring beam. Pier regions at the sides of openings in the walls are also modeled in this manner since it is typically the case that one vertical edge of a pier coincides with an internal partition.
2. The bearing stress on any wall element, and its self-weight, are sufficiently low that any element loaded in-plane will respond in the sliding mode only.
3. The sliding in-plane load-displacement response is nonlinear and assumed to be of elastic-perfectly plastic form.
4. A wall element deforms linearly and elastically before and during sliding.

Zeus-NL of the Mid-America Earthquake Center was selected as the analysis platform based on its automated IDA capabilities (Elnashi et al., 2009). The RC frame and upper storey ring beam were modeled with 3D cubic elasto-plastic beam-column elements which account for the spread of elasticity along member lengths and across section depths (Elnashi et al., 2009). The upper storey slab was modeled as a T-beam in both the longitudinal and transverse directions, with effective slab widths determined based on ACI 318-08 recommendations. Each clay tile masonry wall was modeled as an elastic beam-column, and at each wall-to-support interface a joint element was used to simulate the nonlinear sliding, given point 3 above. Infill walls for structural *Type 3* were modeled with equivalent struts using a bilinear material model based on recommendations by Elnashi (2003) and Kwon (2010). The strengths of these struts were derived from the minimum of either infill panel compression failure or sliding shear failure. The roof diaphragm stiffness in all models was derived from the stiffness of diagonal braces assumed in the roof structure (Naeim, 2001). Mass was applied to the structure with a cubic distributed mass element based on element self- weight and tributary dead load.

In Zeus-NL, material nonlinearity is implemented by using the nonlinear stress-strain relations of possible constituents (Elnashi et al., 2009). Concrete elements, specifically the lower storey frame, upper storey T-beams, and the ring beam, use the Zeus-NL nonlinear constant confinement concrete model. Steel is modeled with a bilinear elasto-plastic material model which includes kinematic strain hardening. Clay tiles and the associated beam-column wall elements utilize an elastic material model with a modulus taken as 3400 MPa based on ASCE 41-06 recommendations (2007).

3. LIMIT STATE DETERMINATION

The limit states for the fragility analysis were determined as the maximum drift of all storeys. Thus, drift was monitored separately during the IDA for both the upper and lower storeys, with the limiting Intensity Measure (IM) value between storeys defining global performance. For upper storey wall elements, the storey drift ratio was selected as the damage measure (DM) for the in-plane response. The four limit

states defined by HAZUS-MH MR4 for the “low-code” case were used to monitor this damage (Hom, 2003). These are: complete damage (CD) – 3.5%, extensive damage (ED) – 1.5%, moderate damage (MD) – 0.5%, and slight damage (SD) – 0.3%. In the out-of-plane direction, the occurrence of dynamic instability (DI) was monitored by comparing the displacement with the displacement capacity, x_c , derived by Priestley (1985) using an energy approach. These criteria are displayed in Table 1.

Table 1: Limit State Determination Criteria

	SD	MD	ED	CD	DI
Upper Storey Drift	0.30%	0.50%	1.50%	3.50%	2.40%
Lower Storey Plastic Column Rotation (radians)	0.005	0.005	0.006	-	-

To determine the interstorey drift limits for the lower storey, local limit states in terms of concrete column plastic rotations were first obtained from ASCE 41-06 (2007). Specifically, the immediate occupancy and life safety performance level rotation limits were taken as 0.005 radians, while the collapse prevention criterion was 0.006 radians. Nonlinear pushover analyses were then performed for each of the three structural models in each horizontal direction using OpenSees, specifically monitoring both beam and column rotations, although beam rotations never controlled the analysis (McKenna and Fenves, 2004). These limit state rotations were then mapped onto the story shear vs. story drift curve, and the global drift limits were defined once a sufficient number of local limits were surpassed. Generally, this was determined once a majority of columns rotated passed a limit state, however judgment was used on a model by model basis. Thus, two drift values were obtained corresponding to rotations of 0.005 and 0.006 radians for each horizontal direction, and for each model.

For this study, immediate occupancy and life safety limit states were assumed to be correlated with slight and moderate damage, respectively, while collapse prevention corresponds to extensive damage. During each dynamic analysis, performance was defined for each limit state as the minimum spectral acceleration value obtained between storeys and between horizontal directions.

4. FRAGILITY ANALYSIS

4.1 Methodology

Fragility is the probability of exceeding a limit state as a function of an intensity measure of the ground shaking. The spectral acceleration, S_a , was selected as the IM as it is thought to require a minimum of ground motion records for the same confidence level (Kumar, 2006). Furthermore, the resulting functions can then be used in probabilistic frameworks that are expected to be adopted for developing risk analysis tools for Caribbean application. If D is the limit state corresponding to a DM, then

$$\text{Probability of exceeding a limit state} = P(\leq D) = \Phi\left[\frac{(\ln(\text{IM}) - \lambda)}{\xi}\right] \quad (4.1)$$

where λ is the mean, μ , of the $\ln(\text{IM})$ and ξ is the standard deviation, σ , of the $\ln(\text{IM})$. This study accounts for both aleatory (record-to-record) and epistemic uncertainties through the EIDA procedure proposed by Dolsek (2009).

4.2 Extended Incremental Dynamic Analysis

EIDA combines IDA with a set of structural models determined through Latin Hypercube Sampling (LHS) and optimized with Simulated Annealing (SA). Aleatory uncertainty is quantified by subjecting the

structural model to a range of ground records, while epistemic uncertainty is accounted for by subjecting a range of structural models to a ground motion record. LHS was selected as the sampling technique based on its improved efficiency over other methods such as Monte Carlo simulation and First-Order Second-Moment (FOSM) reliability analysis (Vamvatsikos and Lignos, 2011). In LHS, variables are sampled from a stratified distribution, and then paired randomly with other variables determined in a similar manner. In this study, sampling with LHS produces an $n \times m$ matrix, with n equal to the number of distribution intervals or samples (N_{sim}), and m equal to the number of random variables (N_{var}). However, LHS tends to introduce undesired correlation between variables, which mandates further optimization of the sample set (Dolsek, 2009).

Simulated Annealing is an optimization algorithm whereby an input vector is continuously modified and an objective function is then checked for improved accuracy over the existing objective function. The objective function described by Dolsek and utilized here is summarized by Eqn. 4.2:

$$E = \frac{2}{N_{var}(N_{var}-1)} \sqrt{\sum_{i=1}^{N_{var}-1} \sum_{j=i+1}^{N_{var}} (S_{i,j} - K_{i,j})^2} \quad (4.2)$$

where N_{var} is the number of variables, $S_{i,j}$ is the generated correlation coefficient between random variables X_i and X_j , and $K_{i,j}$ is the prescribed correlation coefficient between those same variables (Dolsek 2009). The $N_{sim} \times N_{var}$ variable matrix is the input parameter for the algorithm, and this matrix is then modified by the random exchange of two sample values of a single variable. This mutation is accepted if the correlation between variables is smaller as calculated by the objective function, and rejected otherwise.

4.3 Ground Motion Input

The recording of strong ground motions due to earthquakes in the Caribbean is in its infancy; therefore ground acceleration records required as input for dynamic analysis are not readily available. Ten ground motion far-field records from the PEER Strong Motion Database (2009) were arbitrarily selected and their characteristics are shown in Table 2. Each of these was used to derive an artificial accelerogram that is compatible with the IBC 2006 design acceleration response spectrum for Site Class D, and using the (interim) S_s and S_1 2%/50-year maps of the Seismic Research Center of The University of the West Indies, for a site located in the capital city of Port-of-Spain. The artificial accelerograms were calculated using the Kumar algorithm and Spec3 software (Kumar, 2006). An advantage of this approach is that the resulting accelerogram has the same Fourier phases as the PEER records, hence the same (relative) damage potential.

Table 2: Ground Motion Records

Earthquake File	Event Name	Magnitude	PGA (g)	Distance (km)
CPE147	Imperial Valley 79	6.6	0.169	26.5
CPE237	Imperial Valley 79	6.9	0.157	26.5
DSP000	Landers 92	4.4	0.171	23.2
DSP090	Landers 92	7.4	0.154	23.2
JOS000	Landers 92	7.4	0.274	11.6
JOS090	Landers 92	7.4	0.284	11.6
MV000	Landers 92	7.4	0.188	19.3
MV090	Landers 92	6.5	0.140	19.3
NPS000	Landers 92	7.3	0.136	24.2
PT315	Imperial Valley 79	7.4	0.204	14.2

4.4 Determination and Optimization of Structural Model Sets

Of importance in the EIDA procedure is the selection of random variables which accurately reflect modeling uncertainties (Dolsek 2009). Six random variables were considered for uncertainty analysis in this study. These included the steel yield strength (f_y), concrete compressive strength (f'_c), the width of columns and beams (b), the effective slab width in both the longitudinal and transverse directions ($b_{e, long}$ & $b_{e, tran}$), and the clay unit wall modulus (E_c). Additionally, the strength of the infill strut (F_{strut}) was considered as a seventh variable for structural *Type 3*. The random variables and the associated statistical characteristics are shown in Table 3. All variables were assumed to be uncorrelated, and the mean values of each random variable were implemented to form the base models for house *Types 2, 3, and 4*.

Table 3: Random Variable Statistical Properties

Random Variable	Mean Value	COV	Distribution
Steel Strength, f_y	60 ksi	0.05	Normal
Concrete Strength, f'_c	2.9 ksi	0.2	Normal
Masonry Wall Modulus, E_m	495 ksi	0.2	Normal
Beam Width, b	12 in.	0.08	Normal
Effective Slab Width, $b_{e, long}$	32 in.	0.2	Normal
Effective Slab Width, $b_{e, tran}$	42 in.	0.2	Normal
Infill Strut Strength, F_{strut}	14.4 kips	0.2	Normal

To determine an appropriate sample size (N_{sim}) for use in EIDA, a parametric study was conducted over a range of sample sizes. Table 4 displays these results, and a sample size of 15 was chosen for all three structural models. Therefore, for each structural type, 15 additional Zeus-NL mathematical models were created with the sampled properties. E_{max} in Table 4 is the initial value of the objective function prior to optimization, while E is the final optimized value of the objective function. These results show that the SA algorithm for this research provides approximately a 50 times improvement over the un-optimized LHS results. Both LHS and Simulated Annealing were performed with MATLAB.

Table 4: Sample Set Optimization

N_{sim} Optimization for Structural <i>Types 2 and 4</i>						
N_{sim}	6	9	12	15	20	50
E	0.0537	0.0053	0.0018	0.0011	0.0006668	0.000098027
E_{max}	0.1100792	0.0846293	0.0837091	0.0733383	0.0458471	0.031245912
N_{sim} Optimization for Structural <i>Type 3</i>						
N_{sim}	6	9	12	15	20	50
E	0.0566	0.0073	0.0031	0.0016	0.0008053	0.0000716
E_{max}	0.0945444	0.0779115	0.0742807	0.0671503	0.0636983	0.028642405

4.5 Performing EIDA

The EIDA was performed using the Z-Beer utility of Zeus-NL. For the three structural types considered in this study, a base model comprising the mean random variable values shown in Table 3 was analyzed in addition to 15 models created with sampled variables from LHS and the SA algorithm. This corresponds to a total of 48 different structural models, each analyzed with the IDA method by Vamvatsikos and Cornell (2002). For each structural model, the 10 accelerograms were applied in each orthogonal direction, scaled 14 times from 0.3 to 4.2 in increments of 0.3. In all, 48 models were analyzed

for 10 ground motion records applied in 2 directions and scaled 14 times, for a total of 13,440 individual dynamic analyses.

For the limit states of slight, moderate, and extensive damage, performance was monitored in both storeys of the structure. Complete damage and dynamic instability pertain only to the upper storey, and were monitored accordingly. The minimum IM value for an applied accelerogram was selected per limit state, considering both orthogonal directions and both storeys if applicable for that limit state. For each of the three structural types, a maximum of 160 IM values (16 models* 10 accelerograms) contributed to the creation of each fragility curve.

5. RESULTS AND DISCUSSIONS

Figures 4-6 show the fragility curves for house *Types 2* through *4* respectively.

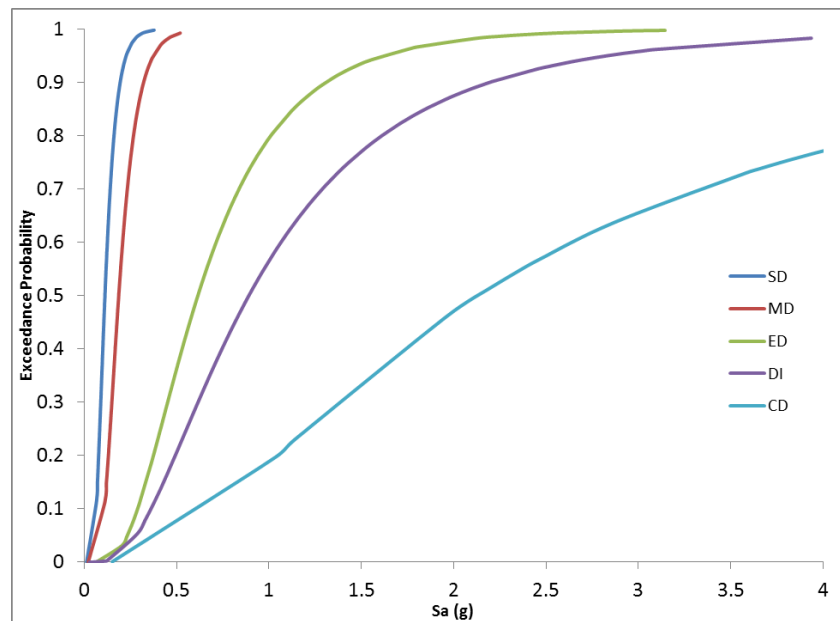


Figure 4. Fragility Curves for House *Type 2*

Based on the fragility curves, house *Type 2* is most vulnerable to damage for a given intensity measure. This is depicted by *Type 2* having a higher exceedance probability for any given limit state and value of S_a than the other structural types. Of importance however, is that the least vulnerable structure for the limit states of slight and moderate damage is house *Type 4*, or the model on the hillside. This can be contributed to an increased stiffness associated the shorter columns further up the hill. For the extensive damage limit state, the most vulnerable structure is again *Type 2*, followed by *Types 4* and then the infill model. The extensive damage limit state is the minimum of 1.5% in-plane upper storey drift, or a column plastic rotation limit of 0.006 radians. However, it is very uncommon for the upper storey in-plane drift to surpass the 1.5% limit, so extensive damage is overwhelmingly controlled by excessive column rotation. Dynamic instability has a lower exceedance probability than extensive damage for both house *Types 2* and *4*, and is thus less likely to occur. However for house *Type 3*, with the infill frames, dynamic instability occurs before excessive damage until a spectral acceleration of approximately 2.5g. This is attributed to the significant increase in column stiffness provided by the infill frames, thus preventing excessive rotations. Finally, complete damage occurs only occasionally for house *Type 2*, and sufficient data could not be collected to create the complete damage fragility curves for *Types 3* and *4*.

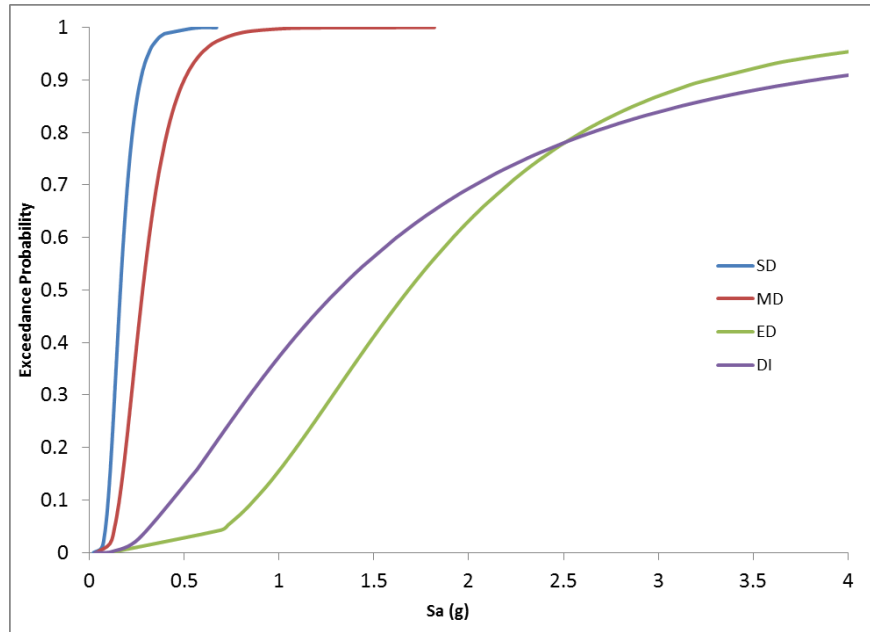


Figure 5. Fragility Curves for House *Type 3*

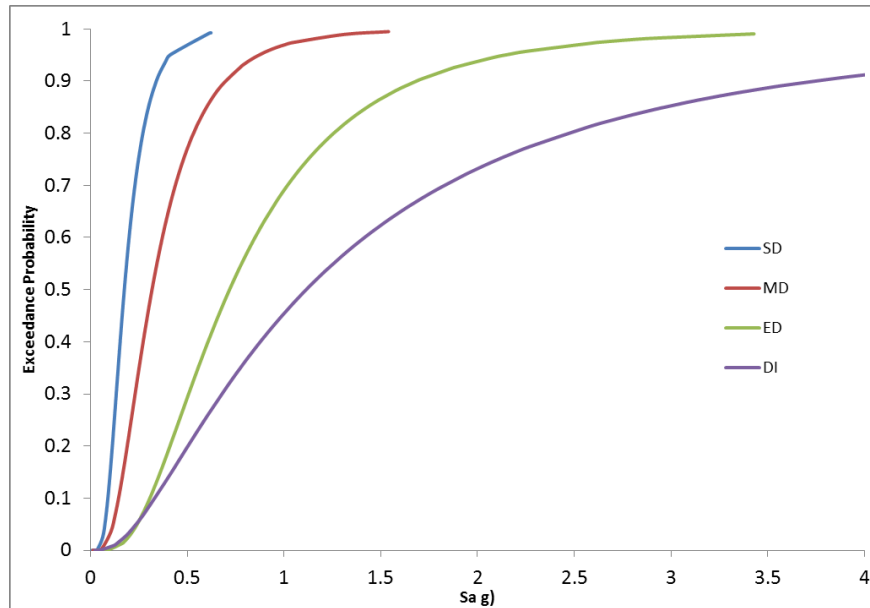


Figure 6. Fragility Curves for House *Type 4*

Though not presented in this paper, in general the shorter direction of the house is more susceptible to in-plane drift damage, which is typical. Out-of-plane dynamic instability occurs almost always in the longer plan direction, which is also to be expected. The physical reason for the dynamic instability is that the masonry walls are very slender and flexible, and have no effective cross-walls to stiffen the response. When dynamic instability occurs, it is likely that the wall elements in the out-of-plane direction will physically disengage from the structure and fall out. This behavior is similar to that of the single-storey residential structures found in Clarke (2010).

6. CONCLUSIONS

The conclusions of this study on the fragility of typical two-storey residential structures in Trinidad and Tobago are as follows:

1. The analytically derived lognormal fragility curves are as presented in Figures 4 through 6 for house *Types 2-4* respectively. House *Type 2* is more susceptible to damage at all limit states than are *Types 3* and *4*. For slight and moderate damage, house *Type 4* is the least vulnerable structure. However, for more severe damage measures, structural *Type 3*, or the infill frame model, is least vulnerable for a given intensity measure.
2. The curves indicate a particular susceptibility to failure by excessive lower storey column rotation coupled with dynamic instability in the out-of-plane direction due to the high flexibility and slenderness of the upper storey URM walls.
3. Given the prevalence of these types of structures in Trinidad and Tobago, this represents a significant threat of large scale economic loss to a developing country which also plays a major role in the economics of the Caribbean as a whole.

REFERENCES

- ACI 318-08, (2008). Building Code Requirements for Structural Concrete and Commentary. *American Concrete Institute*. Farmington Hills, MI.
- ASCE, (2007). ASCE 41-06: Seismic Rehabilitation of Existing Buildings. ASCE.
- Applied Technology Council, (2007). Guidelines for Seismic Performance Assessment of Buildings, ATC-58 35% Draft.
- Clarke, R.P. (1998). The Hysteretic Behavior of Ferrocement-Retrofitted Clay Block Masonry Walls Under In-Plane Reversed Cyclic Lateral Loads: Experimental Investigations and Graphical Computer Models. PhD Thesis. The University of the West Indies, St. Augustine Campus, Trinidad.
- Clarke, R.P. (2010). Seismic Fragility Functions for Typical URM Single-Story Residential Structures in Trinidad and Tobago. *Proceedings of the 9th U.S. National and 10th Canadian Conference on Earthquake Engineering*, July 25-29, 2010, Toronto, Ontario, Canada.
- Dolsek, M. (2009). Incremental dynamic analysis with consideration of modeling uncertainties. *Earthquake Engng. Struct. Dyn.*, **38**: 805–825.
- Elnashi, M., and Erberik, M. (2003). Seismic Vulnerability of Flat-Slab Structures, Technical Report, Mid-America Earthquake Center DS-9 Project. The University of Illinois at Urbana-Champaign.
- Elnashi, A.S., Papanikolaou, V.K, and Lee, D. H. (2009). *Zeus-NL A System for Inelastic Analysis of Structures, Version 1.8.7*. Mid-America Earthquake Center, University of Illinois at Urbana-Champaign.
- Hom, D.B, Poland, and C.D. (2003). ASCE 31-03: Seismic Evaluation of Existing Buildings. ASCE.
- Kumar, A. (2006). Software for Generation of Spectrum Compatible Time History Having Same Phase as of a Given Time History. *Proceedings of the 8th U.S. National Conference on Earthquake Engineering*, April 18-22, San Francisco, California.
- Kwon, O. and Kim, E. (2010). Case Study: Analytical Investigation on the Failure of a Two-Story RC Building Damaged During the 2007 Pisco-Chincha Earthquake. *Engineering Structures*, **32:3**, 1876-1887.
- McKenna, F. and Fenves, G.L. (2004). Open System for Earthquake Engineering Simulation. Pacific Earthquake Engineering Research Center, Berkeley, CA. Available from: <http://opensees.berkeley.edu/>.
- Naeim, F. (2001). The Seismic Design Handbook, 2nd Edition, Kluwer Academic Publishers, Boston, MA.
- PEER Strong Motion Database. Pacific Earthquake Engineering Research Center, Berkeley, California. <http://peer.berkeley.edu/smcat/>.
- Priestley, M.J.N. (1985). Seismic Behaviour of Unreinforced Masonry Walls. *Bull. N.Z. Soc. Earthquake Engineering*, **18:2**, 191-205.
- Vamvatsikos, D, and Cornell, A.C. (2002). Incremental Dynamic Analysis. *Journal of Earthquake Engineering and Structural Dynamics*, **31:3**, 491-514.
- Vamvatsikos, D. and Lignos, D.G. (2011). Evaluating the epistemic uncertainty of the seismic demand and capacity for a 9-story steel moment-resisting frame. *Proceedings of the 7th Hellenic National Conference on Steel Structures*, Volos, Greece.